

NO_x Removal Using Dielectric Barrier Discharges in a Wire-cylinder Pellets-filled Reactor Stressed by High Pulse Voltage

H Wedaa
Assiut University
Egypt
h_wedaa@yahoo.com

M Abdel-Salam
Assiut University
Egypt
mazen2000as@yahoo.com

A Ahmed
Assiut University
Egypt
a_ahmed65@yahoo.de

A Mizuno
Toyohashi University
of Technology
Japan
mizuno@eco.tut.ac.jp

1 Abstract:

This paper is aimed at investigating the nitrogen oxides (NO_x) removal using dielectric barrier discharges (DBD) in a wire-cylinder reactor filled with dielectric pellets and stressed by high pulse voltage. The effects of various parameters (the voltage amplitude, frequency, gas flow rate, and use of dielectric pellets) on the discharge power, NO removal efficiency and NO_x concentration have been studied experimentally. Two dielectric materials (γ -alumina and glass pellets) were evaluated for their ability to reduce NO_x using non-thermal plasma. To reduce the NO_x concentration, the output of the plasma reactor was pumped into sodium sulfite (Na₂ SO₃) solution with different concentrations to absorb NO₂. It has been found that the discharge power and NO removal efficiency increase with the increase of the applied peak voltage and frequency. On the other hand, the discharge power is independent of the gas flow rate, while the NO removal efficiency increases with the decrease of the gas flow rate. The NO_x concentration decreases with the increase of the applied peak voltage, frequency and concentration of Na₂ SO₃ solution, while the NO_x concentration decreases with the decrease of the gas flow rate.

2 Introduction

At atmospheric pressure and room temperature, there are commonly two methods for producing non-thermal plasma (NTP): (i) pulsed corona discharges (PCD) and (ii) dielectric barrier discharges (DBD) [1].

DBD is characterized by the presence of at least one insulating layer (dielectric barrier) between electrodes. The dielectric barrier limits the discharge current, preventing the transition to an arc. This stable discharge that can be generated under atmospheric pressure is suitable for ozone generation [2, 3], NO_x removal [4-6] and SO₂ removal [7].

A combination of plasma and dielectric pellets may improve energy efficiency and selectivity of the plasma chemical processes and packed bed can easily realize this combination [4].

To increase the NO_x removal efficiency, the DBD reactor was supported by heterogeneous catalysts such as selective catalytic reduction (SCR) with ammonia injection [8] or chemical

scrubbers such as sodium sulfite (Na₂SO₃) solution which is used for scrubbing NO₂ [9].

In this study, the effects of various parameters (voltage amplitude, frequency, gas flow rate, and use of the dielectric pellets) on the discharge power and NO/NO_x removal efficiency have been examined experimentally using wire-cylinder reactor. The role of the sodium sulfite solution and its concentrations for NO_x removal has been studied.

3 Experimental Setup

The DBD reactor consists of a stainless discharge wire (diameter: 0.2 mm) extending along the axis of a cylindrical glass tube (inner diameter: 20 mm, outer diameter: 25 mm, length: 350 mm) which was used as the dielectric material. A grounded stainless mesh with a length of 200 mm was wrapped outside the glass tube.

The space between the discharge wire and the glass tube is filled with dielectric pellets of average diameter 3 mm (γ -alumina and glass pellets). The electric field is intensified around

the pellet contact points, causing partial discharges between the pellets. This partial discharge together with the discharge from the discharge wire helps in increasing the production of free radicals required for deNO_x process.

A schematic diagram of the experimental setup is shown in figure 3-1. A pulse generator (ECG-KOKUSAI model PPS-5000) with variable frequency was used for applying the pulsed voltage to the DBD reactor. The applied high voltage was measured using a 1000: 1 high voltage probe (Tektronix P6015A). The discharge current in the reactor was measured using a Rogowski coil (Pearson current monitor model 2877), which was connected in the return current to the ground. The discharge power was calculated based on the time integration of the product of voltage and current waveforms. All waveforms were displayed on a digital oscilloscope (Tektronix TDS 1012B).

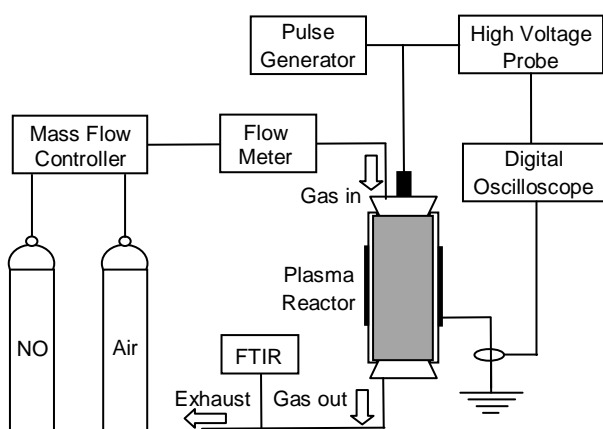


Fig. 3-1: A schematic diagram of the experimental setup

Simulated gas (dry air + NO, N₂ base) was fed through a mass flow controller and flow meter at 5 L/min and the initial concentration of NO was 200 ppm. The experimental measurements were carried out at room temperature under normal pressures with a constant relative humidity (10%).

FTIR (Fourier Transform Infra-Red) spectroscope gas analyzer (model SESAM 3-N) was inserted to measure the concentrations of NO. This model of FTIR is intended to be used for monitoring diesel gas where it requires gas flow rate of minimum of 4 L/min. For 2 L/min flow rate through the reactor, the gas was mixed with 3 L/min of dry air added before the FTIR analysis.

The discharge energy density is usually used to compare NO removal efficiency values at

different discharge volumes, gas residence times, and discharge powers. The discharge energy density is determined as follows in equation (1):

$$E_d = \frac{(P_d \times 60)}{Q} \quad (1)$$

Where E_d, P_d, and Q are the energy density (J/L), discharge power (W), and gas flow rate (L/min), respectively.

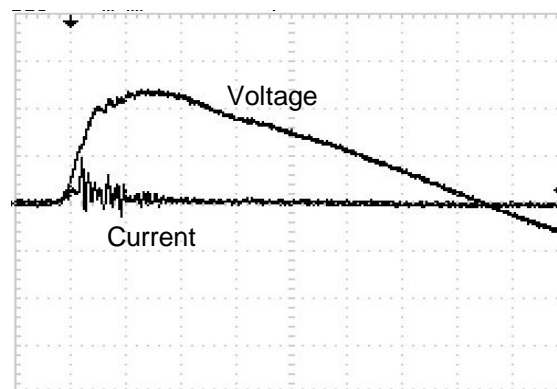
The NO removal efficiency is given in equation (2):

$$\text{NO Rem. Effic.} = \left(\frac{\text{NO}_i - \text{NO}_f}{\text{NO}_i} \right) \times 100 \quad (2)$$

Where NO_i and NO_f are the initial and final concentrations of NO in ppm, respectively.

4 Results and Discussion

Typical waveform oscillograms of the pulsed high voltage and the discharge current are shown in figure 4-1 at peak voltage of 12 kV, frequency of 3 kpps, and flow rate of 5 L/min. The rise time of the pulse voltage was around 430 ns and the fall time up to 50% of the peak value was 2400 ns. The pulse width was about 3700 ns during the first rise pulse.



Voltage [5 kV/div.], Current [1 A/div.], Time [500 ns/div.]

Fig. 4-1: Oscillograms showing the waveforms of the pulsed voltage and the associated discharge current at 12 kV, 3 kpps, and 5L/min

4.1 NO_x Removal Using the γ-Alumina Pellets-filled Reactor

4.1.1 Effect of Applied Voltage Amplitude and Frequency

Figure 4-2 shows the relation between the discharge power and the applied peak voltage

for the γ -alumina pellets-filled reactor at various frequencies (1, 2, 3 kpps) and flow rate of 5 L/min. It is clear that the discharge power increases with the increase of the applied voltage and frequency.

Figure 4-3 shows the NO removal efficiency as a function of the applied peak voltage for the γ -alumina pellets-filled reactor at various frequencies (1, 2, 3 kpps) and flow rate of 5 L/min. It is observed that the NO removal efficiency increases with the increase of the applied voltage and frequency. When the applied voltage or frequency increases, more number of micro discharges per unit time are generated. This results in more production of radicals with a subsequent increase of the NO removal efficiency due to the oxidation of NO to NO₂ by oxygen and ozone radicals (O and O₃). These radicals are produced from the oxygen molecules in the dry air by electron impact.

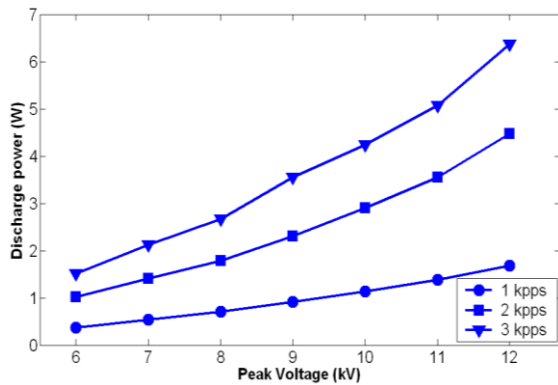


Fig. 4-2: Discharge power as a function of the applied voltage for various frequencies at 5 L/min

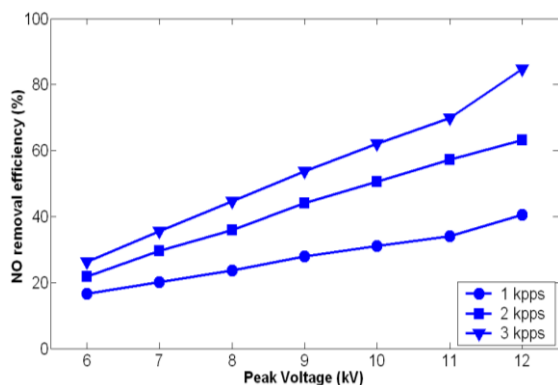


Fig. 4-3: NO removal efficiency as a function of the applied voltage for various frequencies at 5 L/min

Figure 4-4 shows the NO removal efficiency as a function of the energy density for the γ -alumina pellets-filled reactor at various frequencies (1, 2, 3 kpps) and flow rate of 5 L/min. It is clear that the removal efficiency increases with increasing energy density for all

cases, while the maximum removal efficiency increases with increasing the frequency.

Figure 4-5 shows the NO_x concentration in ppm as a function of the applied peak voltage for the γ -alumina pellets-filled reactor at various frequencies (1, 2, 3 kpps) and flow rate of 5 L/min. It is observed that the NO_x concentration decrease with the increase of the applied voltage and frequency. The reduction of NO_x concentration is a result of the ability of γ -alumina pellets to absorb NO₂.

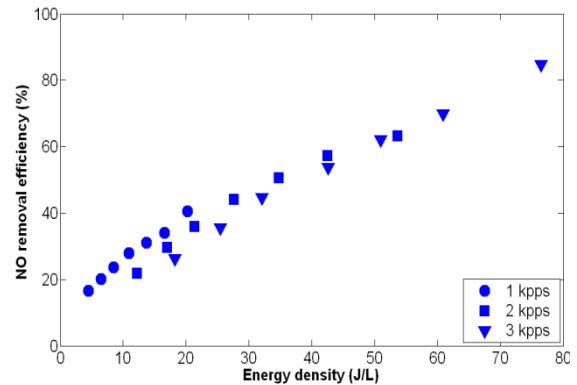


Fig. 4-4: NO removal efficiency as a function of the energy density for various frequencies at 5 L/min

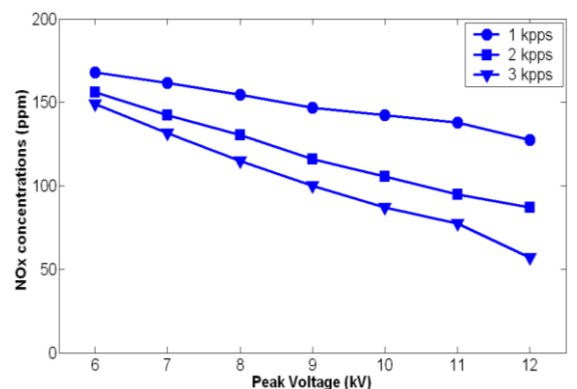


Fig. 4-5: NO_x concentrations as a function of the applied voltage for various frequencies at 5 L/min

4.1.2 Effect of Gas Flow Rate

Figure 4-6 shows the dependency of discharge power on the applied voltage for the γ -alumina pellets-filled reactor at various gas flow rates (2, 5, 10 L/min) and frequency of 2 kpps. It is observed that the discharge power is independent of the value of the gas flow rate while it increases with the increase of the applied voltage for all cases.

Figure 4-7 shows the NO removal efficiency as a function of the applied peak value of the applied voltage for the γ -alumina pellets-filled reactor at various flow rates (2, 5, 10 L/min) and frequency of 2 kpps. It is clear that the NO

removal efficiency increases with the decrease of gas flow rate due to the increase of residence time of the gas within the volume of the reactor.

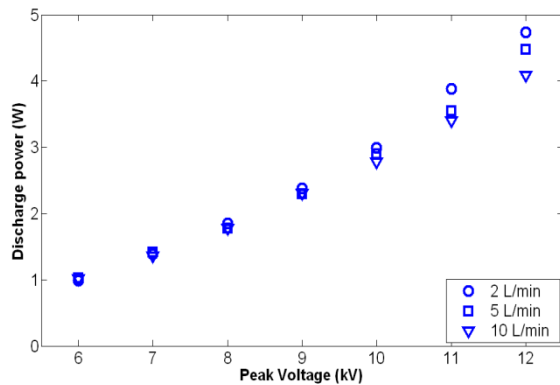


Fig. 4-6: Discharge power as a function of the applied voltage for different gas flow rates at 2 kpps

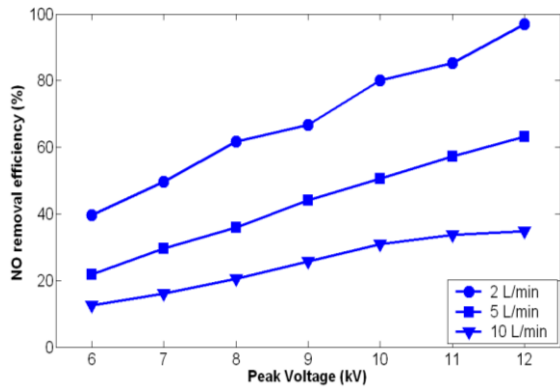


Fig. 4-7: NO removal efficiency as a function of the applied voltage for different flow rates at 2 kpps

Figure 4-8 shows the NO removal efficiency as a function of the energy density for the γ -alumina pellets-filled reactor at various flow rates (2, 5, 10 L/min) and frequency of 2 kpps. The removal efficiency increases with the increase of the energy density for all gas flow rates. The maximum removal efficiency increases with the decrease of the gas flow rate, while the removal efficiency at the same energy density remains the same at different flow rates.

Figure 4-9 shows the NO_x concentration as a function of the applied peak value of the applied voltage for the γ -alumina pellets-filled reactor at different gas flow rates (2, 5, 10 L/min) and frequency of 2 kpps. It is observed that the NO_x concentration decrease with the decrease of the gas flow rate and the increase of the applied voltage. At lower gas flow rate, the ability of γ -alumina pellets to absorb NO₂ increases due to the increase of residence time of the gas within the reactor volume.

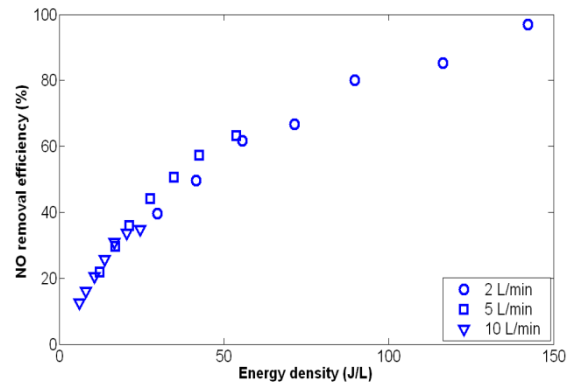


Fig. 4-8: NO removal efficiency as a function of the energy density for different flow rates at 2 kpps

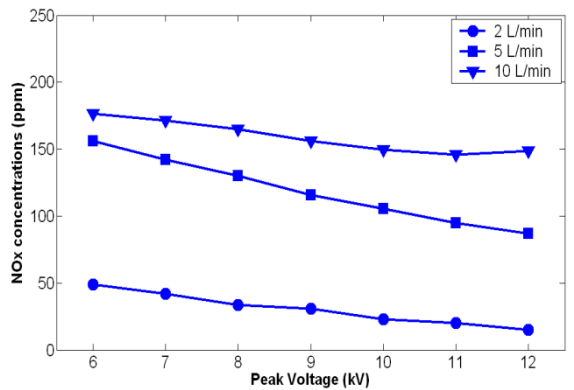


Fig. 4-9: NO_x concentrations as a function of the applied voltage for different flow rates at 2 kpps

4.1.3 Effect of Dielectric Pellets

Figure 4-10 shows the dependency of discharge power on the peak value of the applied voltage without and with pellets (γ -alumina and glass pellets) at frequency of 2 kpps and flow rate of 5 L/min. It is observed the discharge power increases with the increase of the peak voltage for all cases in figure 4-10 and assumes the highest values on using γ -alumina pellets.

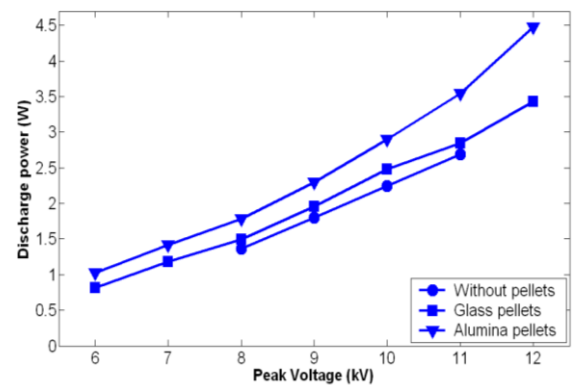


Fig. 4-10: Discharge power as a function of the applied voltage with and without pellets at 2 kpps and 5 L/min

Figure 4-11 shows the NO removal efficiency as a function of the peak value of the applied voltage without and with pellets (γ -alumina and glass pellets) at frequency of 2 kpps and flow rate of 5 L/min. It is clear that the removal efficiency increases with the increase of the peak voltage for all cases in figure 4-11 and assumes the highest values on using γ -alumina pellets.

Figure 4-12 shows the NO removal efficiency as a function of the energy density without and with pellets (γ -alumina and glass pellets) at frequency of 2 kpps and flow rate of 5 L/min. It is clear that the removal efficiency increases with the increase of the energy density for all cases in figure 4-12 and assumes the highest values on using γ -alumina pellets.

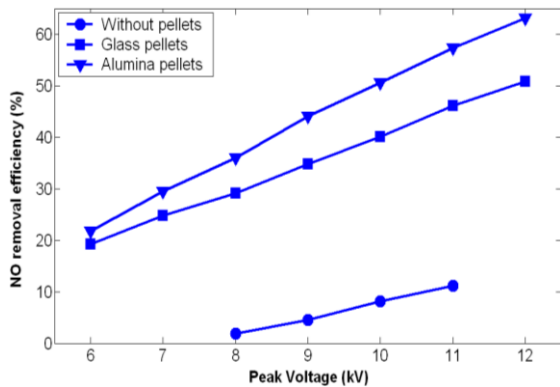


Fig. 4-11: NO removal efficiency as a function of the applied voltage with and without pellets at 2 kpps and 5 L/min

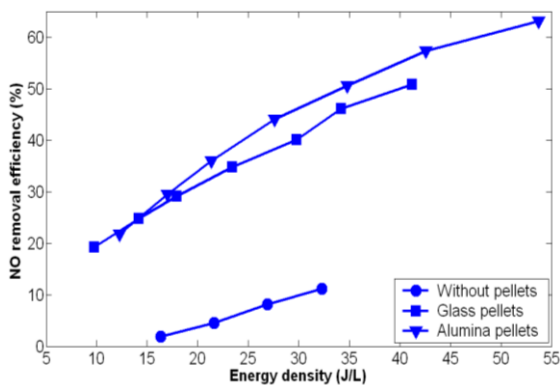


Fig. 4-12: NO removal efficiency as a function of the energy density with and without pellets at 2 kpps and 5 L/min

Figure 4-13 shows the NO_x concentration as a function of the applied peak voltage without and with pellets (γ -alumina and glass pellets) at frequency of 2 kpps and flow rate of 5 L/min. It is observed that the γ -alumina pellets give best performance for removing NO_x when compared to other cases in figure 4-13. This is attributed to the capability of the γ -alumina

pellets in removing NO_x by oxidation of NO and absorption of the resulting NO₂. On the other hand, glass pellets can reduce NO by oxidation as shown in figure 4-11 and NO_x concentration increases with values more than the initial value of NO_x (=200 ppm), figure 4-13. This means that the glass pellets has no ability to absorb NO₂.

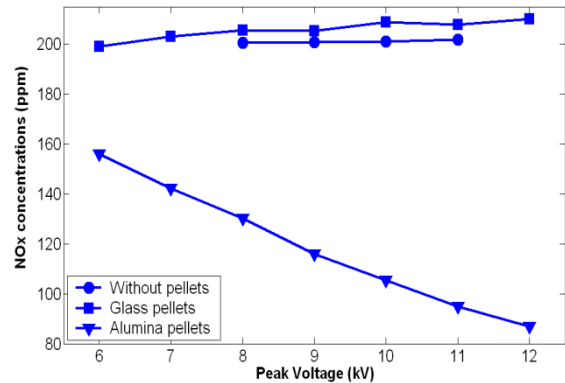


Fig. 4-13: NO_x concentrations as a function of the applied voltage with and without pellets at 2 kpps and 5 L/min

4.2 Improvement of NO_x Removal of Glass Pellets-filled Reactor

To reduce the NO_x concentration, the glass pellets-filled reactor is followed by sodium sulfite (Na₂ SO₃) solution with different concentration to absorb NO₂ resulting from the oxidation process within the reactor (NO to NO₂).

Figure 4-14 shows the temporal variation of the NO_x concentration for the glass pellets-filled reactor at peak voltage of 10 kV, flow rate of 5 L/min, frequency of 2 kpps and concentration of Na₂ SO₃ solution of 126g/L.

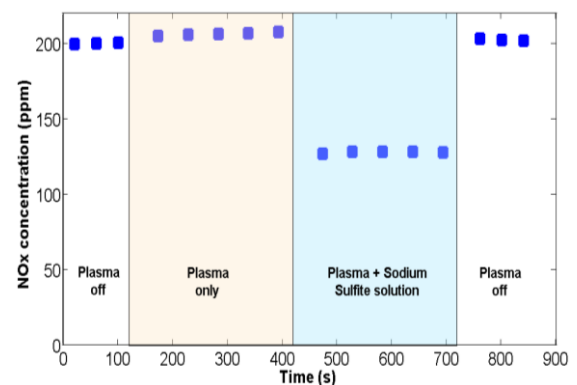


Fig. 4-14: Temporal variation of NO_x concentration for the glass pellets-filled reactor at 10 kV, 5 L/min, 2 kpps and 126 g/L

From figure 4-14, it is clear that the glass pellets-filled reactor has no effect on NO_x

concentration due to the balance between the decrease of NO and the increase of NO₂. On the other hand, the glass pellets-filled reactor followed by Na₂ SO₃ solution reduces the NO_x concentration due to ability of the solution to absorb NO₂.

Figure 4-15 shows the NO_x concentration as a function of the applied peak voltage for the glass pellets-filled reactor at flow rate of 5 L/min, frequency of 2 kpps and different concentrations of Na₂ SO₃ solution (25.2, 126, 252 g/L). The NO_x concentration decreases with the increase of the concentration of sodium sulfite solution due to increasing the ability of the solution to absorb NO₂.

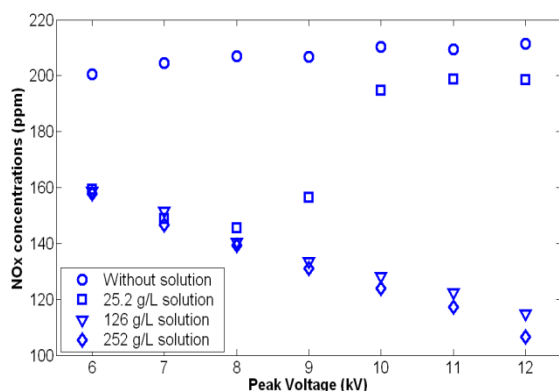


Fig. 4-15: NO_x concentration as a function of the applied voltage for the glass pellets-filled reactor at 5 L/min, 2 kpps and different concentration of Na₂ SO₃ solution

5 Conclusion

NO_x removal using dielectric barrier discharge in a wire-cylinder pellets-filled reactor stressed by high pulse voltage was investigated. Two dielectric materials (γ-alumina and glass pellets) were evaluated for their ability to reduce NO_x using non-thermal plasma. The role of sodium sulfite solution with different concentrations for reducing the NO_x concentration was studied. The discharge power and NO removal efficiency increase with the increase of the applied peak voltage and frequency. On the other hand, the discharge power is independent of the flow rate, while the NO removal efficiency increases with decreasing flow rate. The γ-alumina pellets give the best performance for removing NO_x when compared with other cases due to their ability to oxidize NO to NO₂ and absorb the resulting NO₂. The NO_x concentration decreases with the increase of the applied voltage, frequency and concentration of Na₂ SO₃ solution, while it decreases with the decrease of the flow rate.

6 Literature

- [1] B. Pashaie, S. K. Dhali, and F. I. Honea, "Electrical characteristics of a coaxial dielectric barrier discharge", *Journal of Physics D: Applied Physics*, Vol. 27, No. 10, 1994, pp. 2107-2110.
- [2] Z. Fang, Y. Qiu, Y. Sun, H. Wang, and K. Edmund, "Experimental study on discharge characteristics and ozone generation of dielectric barrier discharge in a cylinder-cylinder reactor and a wire-cylinder reactor", *Journal of Electrostatics*, Vol. 66, 2008, pp. 421-426.
- [3] M. Abdel-Salam, A. Hashem, A. Yehia, A. Mizuno, A. Turky, and A. Gabr, "Characteristics of corona and silent discharges as influenced by geometry of the discharge reactor", *Journal of Physics D: Applied Physics*, Vol. 36, 2003, pp. 252-260.
- [4] A. D. Srinivasan and B. S. Rajanikanth, "Nonthermal-Plasma-Promoted Catalysis for the Removal of NO_x From a Stationary Diesel-Engine Exhaust", *IEEE Transactions on Industry Applications*, Vol. 43, No. 6, 2007, pp. 1507 - 1514.
- [5] B.S. Rajanikanth, and V. Ravi, "Pulsed Electrical Discharges Assisted by Dielectric Pellets/Catalysts for Diesel Engine Exhaust Treatment", *IEEE Transactions on Dielectrics and Electrical Insulation*, Vol. 9, 2002, pp. 616-626.
- [6] K. Takaki, M. Shimizu, S. Mukaigawa, and T. Fujiwara, "Effect of Electrode Shape in Dielectric Barrier Discharge Plasma Reactor for NO_x Removal", *IEEE Transactions on Plasma Science*, Vol. 32, No.1, 2004, pp. 32-38.
- [7] H. Ma, P. Chen, M. Zhang, X. Lin and R. Ruan, "Study of SO₂ removal using non-thermal plasma induced by dielectric barrier discharge (DBD)", *Plasma Chemistry and Plasma Processing*, Vol. 22, No. 2, 2002, pp. 239-254.
- [8] C. Ciardelli, I. Nova, E. Tronconi, D. Chatterjee, T. Burkhardt, and M. Weibel, "NH₃ SCR of NO_x for diesel exhausts after treatment: role of NO₂ in catalytic mechanism, unsteady kinetics and monolith converter modeling", *Journal of Chemical Engineering Science*, Vol. 6, 2007, pp. 5001-5006.
- [9] H. Fujishima, A. Tatsumi, T. Kuroki, A. Tanaka, K. Otsuka, T. Yamamoto, and M. Okubo, "Improvement in NO_x Removal Performance of the Pilot-Scale Boiler Emission Control System Using an Indirect Plasma-Chemical Process", *IEEE Transactions on Industry Applications*, Vol. 46, No. 5, 2010, pp. 1722-1729.